J. B. R. Loureiro and
A. P. Silva Freire

Programa de Engenharia Mecânica
Universidade Federal do Rio de Janeiro
PEM/COPPE/UFRJ
C. P. 68503
21.945-970, Rio de Janeiro, RJ, Brazil.
jbrloureiro@mecanica.coppe.ufrj.br
atila@mecanica.coppe.ufrj.br

Experimental Investigation of Turbulent Boundary Layers over Steep Two-dimensional Elevations

This work presents a laboratory study of the behaviour of turbulent boundary layers over steep topographic elevations. Two main topics of interest are addressed here: (i) to investigate and characterize the separated flow region which is formed on the leeside of the elevation, and (ii) to evaluate the effects of flow stability conditions on the properties of boundary layers subjected to surface elevation. To carry out this task, water channel and wind-tunnel investigations were conducted. For the former case, a neutrally stratified boundary layer was simulated in the water-channel of the Hydraulics Laboratory (FEUP). Mean and turbulent velocities were measured through laser-Doppler anemometry. Results provided a thorough description of the inner layers along the hill and inside the recirculation region. The refined near-wall data has contributed to the calculation of the friction velocity along the hill through different methods. For the latter case, neutral, stable and unstable boundary layers were simulated in the wind-tunnel of the Laboratory of Turbulence Mechanics (COPPE/UFRJ). Simultaneous velocity and temperature fields were measured with the aid of thermal anemometry. These results allowed the characterization of the effects of the stratification on the speed-up factor, i.e. the maximum acceleration of the flow on hilltop. The present paper has originally introduced the concept of the heat up/down factor, in order to study the behaviour of the temperature field on the crest of the elevation.

Keywords: *Flow over hills, turbulence, separation, stratification, hot-wire anemometry, laser-Doppler anemometry.*

Introduction

The atmospheric boundary layer is a difficult problem to be modelled and predicted. The warming of the ground by sunlight together with the cooling by nocturnal radiation, the changes in surface elevation, the surface roughness variation, the rotation of the Earth, name only a few of a myriad of conditions that influence the behaviour of atmospheric flows.

The present work investigates two of these conditions: changes in surface elevation and changes in atmospheric stability conditions. In particular, in this study, the main concern is to investigate the effects that a large topographical elevation exerts on the properties of the atmospheric boundary layer.

The primary response of the boundary layer to a change in topography is the acceleration of the flow over the hill crest followed by an associated deceleration on the lee side. Many studies on flows over hills have focused on modeling the behaviour of the speed up factor subject to different surface elevations. An important contribution has been achieved through the linear theory proposed by Jackson and Hunt (1975) for a neutrally stratified boundary layer, which has been further extended in Hunt et al. (1988a) to account for stability effects of the atmosphere. This theory has allowed for rapid calculations of the flow over lower topography, providing a general picture of the perturbed velocity field.

However, when the hill becomes steep enough to form large downstream recirculation region, the validity of this linear framework is severely limited. The major difficulty introduced by the steep elevations is the significant enhancement of the nonlinear effects, introduced by the presence of flow separation. Under such condition, the linear theory is no longer useful for predicting either the mean or the turbulent fields.

In turbulent flows, the mechanism of flow separation is yet poorly understood so that the classical logarithmic expressions used to represent the flow in the near wall region do not find their counterpart near the separation point and in the reverse flow region. Indeed, to this date, there is no established theory capable of accounting for the influence of steep topography on the flow field, especially when considering the behaviour of the turbulent structure.

The combined effects of ground characteristics and of flow stability give rise to many complex atmospheric problems. Since many sources of air pollution are located in complex terrain, detailed and accurate information about the temperature and the flow field are needed so that reasonable predictions of gas concentration can be made. A typical example is the formation of large recirculating flow regions within valleys, where atmospheric conditions may prevent the diffusion of pollutants into the outer atmosphere.

This paper examines problems associated with this motivation. Basically, our two main concerns are: (i) to experimentally investigate the influence of the separation region on the behaviour of the mean and turbulent velocity fields along the topography under neutral condition, and (ii) to evaluate the effects of atmospheric stability conditions on the properties of the boundary layer.

In regard to the first objective, to investigate the characteristics of a separated flow region, a neutrally stratified flow over a steep hill has been simulated in the water-channel of the Laboratory of Hydraulics, of the University of Oporto, Portugal. Measurements of longitudinal and vertical components of mean velocity and its fluctuation components were performed with the aid of laser Doppler anemometry. Refined data were obtained particularly inside the recirculation region.

As for the second objective, wind-tunnel simulations of neutral, stable and unstable boundary layers over a steep model hill have been conducted at the Laboratory of Turbulence Mechanics (COPPE/UFRJ). A two-channel hot-wire system was used so that two components of the mean velocity field and of its fluctuations were obtained outside of the reverse flow region. The temperature data was simultaneously obtained trough a cold-wire anemometer. A flow visualisation study was conducted in order to estimate the onset and location of the recirculation region.

The idea behind the conception of this experimental research is in fact quite simple, to profit from the advantages of each set of experimental apparatus and instrumentation. Thermal anemometry is widely recognised as the most appropriate experimental technique to probe turbulent flows, despite its limitations to resolve the direction of the velocity vector. In addition, thermal stratification applied to wind-tunnel environments is a low-cost and simple way

of achieving good similarity condition with actual atmospheric flows.

On the other hand, laser-Doppler anemometry is easily applied to water flows, and is capable of resolving the velocity direction with a good temporal and spatial resolution. The stability simulation, however, is a great deal more complicated in a water flow environment. Considering that the stratification effect is generally introduced by salty solutions of different concentrations, it becomes unfeasible to maintain a constant stability condition in a closed loop water-channel system.

This paper is organized as follows: the next section provides the reader with a short literature review, in order to give an idea of the recent developments in this field of knowledge. Results will be presented in the following two sections; the first is dedicated to the water-channel experiments, and the second to the wind-tunnel study. Next, post-processed results from the data are introduced and explained; a comparison between the two experiments is made also made here. Conclusions are drawn in the last section, summarizing the main findings and suggesting new studies as future plans.

In general, mean velocity and temperature results are compared with the predictions of the linear theory of Jackson and Hunt (1975), and with the stability corrections proposed by Hunt et al. (1998a). The turbulent flow field is analysed on the basis of the local equilibrium concept and the rapid distortion theory, introduced by Batchelor and Proudman (1954) and described by Townsend (1976). The present results allow a thorough description of the inner region of the boundary layer, extending from the upstream region, along into the separated zone to the downstream lee side. The flow visualization study was quite enriching since it furnished a qualitative location of the separation point and the extension of the recirculation region.

Brief comments on previous works

Arguably, one of the most significant contributions to the comprehension of flow over hills was introduced by Hunt and his co-workers. Based on the asymptotic structure of the boundary layer, Jackson and Hunt (1975) derived a set of linearised equations which can satisfactorily predict the neutral flow over low to moderate surface elevations.

About the same time, and using a similar approach, Sykes (1978) extended the classical triple-deck theory to include the effects of stable stratification in the free-stream flow over the hill. Sykes' linearised solutions were valid only for small hills, but the results indicated that separation could be inhibited under stable free-stream conditions.

Most of the subsequent works have addressed the study of flow and dispersion over low and moderate hill, but focused almost entirely on the behaviour of the speed up factor, e.g. Castro and Snyder (1982), Carruthers and Choularton (1982), Teunissen (1983), Bowen (1983), Arya and Gadiyaram (1986), Arya et al. (1987). Certainly, the interest raised by the demand in understanding the dynamics of pollutant's dispersion as well as optimizing the location of wind energy generators in hilly terrain have steered the course of those researches.

In an original work, Britter et al. (1981) studied the influence of surface roughness and of separation on the characteristics of the "speed up" factor, i.e. the maximum increase in velocity at the hill top. Britter and his co-workers conducted wind tunnel measurements along a two-dimensional hill, which followed a curve of Agnesi profile. The authors found that the perturbation velocity on the hill top could be estimated by assuming a linear superposition of the velocity changes produced by the changes in elevation and in surface roughness. In the lee side, however, this assumption was not valid since the separation region significantly altered the flow characteristics. As for the turbulent structure, Britter et al. (1981) were the first to correlate the fluctuation field to the effects of rapid distortion theory.

Bradley (1980) and Britter et al. (1981) can be considered some of the pioneers in trying to explain the behaviour of the turbulent field over hills. One of the first extensive field measurement campaigns was conducted Bradley (1980). Data were presented for the mean velocity field and turbulent components over Black Mountain, located in Canada. Calculations for the speed up factor were compared with the linear theory of Jackson e Hunt (1975), and an extensive analysis of the behaviour of the turbulent flow field over the elevation has been shown. The turbulent fluctuations were found to behave accordingly to rapid distortion theory, Batchelor and Proudman (1954). Bradley has observed some discrepancies between the measured data and the numerical predictions of Taylor (1977), which could not represent correctly the non-equilibrium region of the flow.

Zeman and Jensen (1987) have developed a new model to investigate the turbulent flow field over two-dimensional hills. They applied the von Mises transformation to the mean momentum equations, along with a second-order turbulence closure type. The model predictions were compared with some experimental results from the Askervein Hill project showing good agreement. The hill perturbation pressure was calculated by means of potential flow theory. The authors focused their attention on the turbulence characteristics of the flow field over hills. They observed that in a region close to the ground the magnitudes of all non-zero stress components are increased relative to the upstream values, in accordance with the increase in mean velocity and shear. At higher levels the effects of rapid distortion of turbulence were found to decrease the magnitude of the longitudinal fluctuations while increasing the vertical fluctuation component. As Mason and King (1985), Zeman and Jensen (1987) have observed some discrepancies in the behaviour of the fluctuation components between different works available in literature. The authors speculated that this fact is due to the upstream anisotropy of the flow, but no further research was conducted to prove this assertion.

A wide perspective on the state of the art of research on atmospheric boundary layers can be obtained from Kaimal and Finnigan (1994), and Belcher and Hunt (1998). These authors point out the main limitation of field investigations on separated flows on the lee side of steep hills: the recirculation depth is usually of the order of hill height, which is just too large to be explored by meteorological towers of field campaigns. From this perspective, wind tunnel studies still have much to contribute to the understanding of separation process in atmosphere.

In regard to stratification effects, wind tunnel experiments by Meroney and Cermak (1975) and by Ogawa et al. (1985) have revealed the main features of the phenomenon for flat terrain. For complex terrain under neutral and stably stratified conditions, Ohba et al. (1990) and Ohya et al. (1994) have also carried wind tunnel simulations with the purpose of studying the diffusion of gas.

In strong stability conditions, the linear approximations referenced above are not valid anymore. For the three-dimensional case, in order to determine the amount of fluid that would flow over a hill instead of around it, Sheppard (1956) advanced some simple energy arguments. Considering the amount of kinetic energy that a fluid parcel would have to have to overcome the potential energy required to lift itself from its upstream height to the top of the hill, he was able to find an expression for the dividing streamline, the streamline that separates those parcels of fluid which pass around the hill from those that pass over the hill. Some authors have tried to improve Sheppard's solution, e.g. Smith (1990), however, it has been demonstrated that the simple expression of Sheppard matches very well laboratory and field data (Snyder et al. (1985)).

For two-dimensional hills, if the flow is unable to pass over the hill it cannot pass around it. In this circumstance, the flow will be trapped below the height of the dividing streamline. Before this situation is achieved, the occurring non-linear flow patterns can be analysed through the shallow water equations for supercritical and subcritical flows; hydraulic jumps and abrupt turbulent transitions

can also occur. All these aspects are discussed in Lamb and Britter (1984).

In moderately stable conditions, the winds are stronger and the natural wavelength of air parcels compare with the size of the hill. Because very few experimental data are available, the behaviour of moderately stable flows is mainly appreciated by theoretical studies. The linearized inviscid equation for the mean vertical velocity together with the theory of Hunt et al.(1988b) are commonly used to calculate the speedup in the inner and middle layers. When this is made for flows over a two-dimensional ridge, results show that for Froude number based on the characteristic length of the hill, F_L between 2 and infinity, little change is observed over the neutral conditions. With F_L increased to 0.33 and 0.5, the speedup on the hillcrest is reduced and strong wind speed maximum on the downwind side of the hill is observed.

For weak stability conditions, the winds are even stronger and the natural wavelength of air parcels is longer than the size of the hill; the flow separates at the lee of the hill creating a large bubble of recirculating flow. Under weakly stable conditions, linear theories can be used. Again, the linear theory of Hunt et al. (1988b) can be invoked provided they are changed by inserting the Monin-Obukhov diabatic corrections. The modified equations are shown (Kaimal and Finnigan (1994)) to work well for values of $F_L \cong 1.5$.

Weak and moderate instabilities can also have the speedup calculated through Hunt et al.'s theory (Hunt et al. (1988a,1988b)) by inserting the Monin-Obukhov corrections into the equations. The changes in speedup are much less significant for unstable flows attaining a constant value of about 0.44. Under unstable conditions the mixing of the flow tends to impose a zero shear condition on the flow which decreases the speedup value.

Strong instability conditions are met only under the very special condition of very small and negative values of the Monin-Obukhov length. With actual values of wall heat flux, this is bound to occur only at times of almost zero mean wind speed. Although this flow has been observed in nature, no data are available which provide a good account of it. Actually, as reminded by Carruthers and Hunt (1990), most of the work found in literature has been dedicated to the study of stable atmospheric conditions.

More recently, Ohba et al. (2002) have performed a wind tunnel study of gas diffusion over an isolated hill under neutral, stable and unstable atmosphere. To every stability condition, typical flow characteristics were noticed. Under neutral conditions, reversed vortices were observed. In stable and unstable conditions, downward slope winds and convective motions were respectively observed. Velocity measurements were made with a laser Doppler anemometer. Methane was used as a tracer gas for dispersion measurements. Since the authors' main objective was to investigate a scalar diffusion, no further attention was given to the velocity field, and only longitudinal mean and turbulence intensity profiles were presented.

During the 90's, the scientific community was witnessing a remarkable growth in computer power and hence, many researchers were led to believe that, in a near future, all complex fluid mechanics problem would be solved numerically. Consequently, one can observe that most of the studies performed during this decade have put their efforts in attempts to predict flow over hills through numerical simulation. Unfortunately, in spite of all the development in computational capabilities, the majority of the models still fail to accurately predict the turbulent field.

Ross et al. (2004), have performed numerical and experimental studies in order to asses the performance of different turbulence closure schemes in predicting the flow field over a hill. Two dimensional steep hills of different slopes, in both neutral and stably stratified flow conditions were studied. Turbulence models that used one-and-a-half and second-order closure schemes were used to predict the mean and turbulent quantities of the flow. The numerical predictions were compared with the wind tunnel experiments. One the authors' conclusion is that none of the turbulence schemes,

including the second-order models, succeeded in providing a good prediction of turbulent quantities.

Given this brief outline of the research regarding flows over hills, the present work has striven to contribute to a better understanding of the problem by generating an extensive and detailed set of experimental data.

Water-channel Experiments

In this section we proceed to the description and the presentation of the results obtained in the former part of this study. Our main concern now is to investigate the properties of a neutrally stratified boundary layer over a steep topography, with a view to study the influence of the separation region on the whole flow field.

Description of the Apparatus and Instrumentation

Several researchers have resorted to water experimentation in order to examine the flow over hills and other obstacles. The towing tank method has been extensively used in the past, as reported by the works of Long (1959), Snyder et al. (1985) and more recently by Gyüre and Jánosi (2003). Indeed, this method is quite appropriate when considering atmospheric flows dominated by blocking, lee waves, inversions and strong stratification effects. However, as explained by Meroney (1990), the towing tank method may distort surface layer predictions because the simulated uniform incoming profile is not equivalent to the shear flows encountered near the earth's surface. Water-channel experiments, on the other hand, do not suffer from this weakness. The mean and turbulent boundary layer profile can be accurately reproduced in this facility. The ratios of longitudinal and vertical fluctuation components of the simulated inner layer are comparable to atmospheric data, as further presented in the results section.

Figure 1. Illustration of water-channel.

The water flow experiments were performed in the open-channel of the Hydraulics Laboratory of the Civil Engineering Department, University of Oporto, Portugal. This water-channel is a 17 m long channel and has a cross section of 40 cm width per 60 cm height. The recirculation system has two underground tanks, an upper stabilizing tank, and four pumps with a maximum total capacity of 150 l/s. The working section has glass side walls, 3 m in length, and was situated 7.3 m downstream of the channel entrance. The model hill was located 8 m from the channel entrance. An illustration of the water channel is presented in Figure 1.

In a typical experimental campaign, two pumps were turned on so as to keep the system running in a steady state, with a maximum flow rate variation of ± 0.8 %. At the entrance of the channel, flow stabilization and uniformization, with the suppression of any excessive level of turbulence, was achieved with the use of a series of screens and filters. These were also used to control the grain-size

of the particles in suspension in the water. A uniform flow rate control was obtained through a magnetic flowmeter, which was installed in the supply line. The water depth along the channel was controlled by a vertical steel gate.

A one component, fiber optic, Dantec laser-Doppler anemometry system was used in the forward scatter mode to measure the mean and the fluctuating velocity fields. The laser source was a 2W Ar-ion operating in multi-mode. A Bragg cell unit was used to introduce an electronic shift of 0.6 MHz. This procedure permitted the resolution of the direction of the flow field and the correct measurement of near-zero mean velocities. Front lenses with 310 mm focal length were mounted on the probe in order to accurately position the measurement volume on the centreline of the channel.

Before collection by the photomultiplier, the scattered light passed through an interference filter of 514.5 nm, so that only green light was acquired. The signal from the photomultiplier was band-pass filtered and processed by a TSI 1990C Counter, operating in single measurement per burst mode. A series of LDA biases were avoided by adjusting the strictest parameters on the data processor. For each point measured, a sample size of 10,000 values has been considered. Table 1 lists the main characteristics of the laser-Doppler system used.

This whole system was used to measure both the longitudinal and the vertical velocity components. This could be done simply by turning the probe around its axis, so that on both conditions, the fringe distribution was perpendicular to the measured velocity component. Typical uncertainties associated to the mean and fluctuating velocity data, U, W, <u'u'>, <w'w'>, <u'w'>, were estimated in $\pm$ 2.5 %, $\pm$ 10 %, $\pm$ 6.5 %, $\pm$ 6.5 % and $\pm$ 12 % respectively.

Laser wavelength	514.5 nm
Measured half angle of the beams	3.415°
Fringe spacing	4.3183 μm
Frequency shift	0.60 MHz
Dimensions of the measurement volume:	
Major axis	2.53 mm
Minor axis	162.0 μm

Table 1. Main characteristics of the laser-Doppler anemometer in air at e^{-2} intensity.

Characteristics of the Model Hill

The model used in the present work was two-dimensional, axisymmetric and aerodynamically smooth. Its geometry was chosen so as to simulate a steep hill which would generate a large recirculation region on its lee side. Based on the works of Britter et al. (1981) and of Arya et al. (1987), the shape of the hill followed a modified "Witch of Agnesi" profile, according to the Equation 1.

$$z = \frac{H_1}{1+\left(\dfrac{x}{L_H}\right)^2} - H_2. \tag{1}$$

Characteristic height	H_1	75 mm
Characteristic height	H_2	15 mm
Hill height	H	60 mm
Hill length	L	600 mm
Characteristic length	L_H	150 mm
Aspect ratio	ar	5
Maximum slope	θ_{max}	18.6°

Table 2. Geometric characteristics of the hill.

Thus, it follows that H ($=H_1-H_2$)($= 60$ mm) is the hill height and L_H ($= 150$ mm) is the characteristic length of the hill representing the distance from the crest to the half-height point. Co-ordinates x and z represent the longitudinal and the vertical axes, respectively. The characteristic parameters of hill are presented in Table 2, where ar denotes the aspect ratio $(L/2)/H$ and θ_{max} the maximum slope.

Two models of equal geometry and proportions have been built for the present study. For the water-channel experiments, the model was built using polished Plexiglass. An illustration of the model hill inside the water-channel is shown in Figure 2.
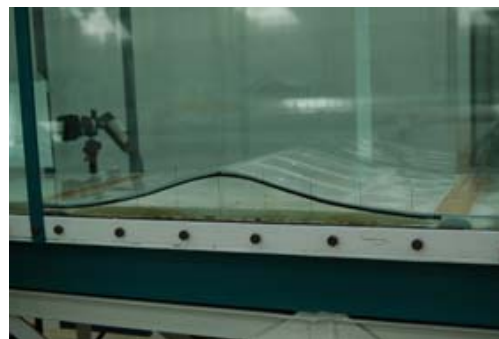

Figure 2. Model of the topographic elevation inside the water-channel.

Measurement Conditions

Measurements were performed for thirteen stations along the model hill. Figure 3 shows the spatial distribution of the measured profiles.

All the profiles were measured at the centerline of the water-channel, at a flow rate of 4.0 l/s and water height of 236 mm.

For the longitudinal velocity component measurement, data was acquired as near as 0.25 mm from the wall. The vertical velocity component and the shear stress terms could only be measured from approximately 5 to 7 mm from the wall, since at such configurations the laser beams would reach the wall before crossing at the measurement volume.
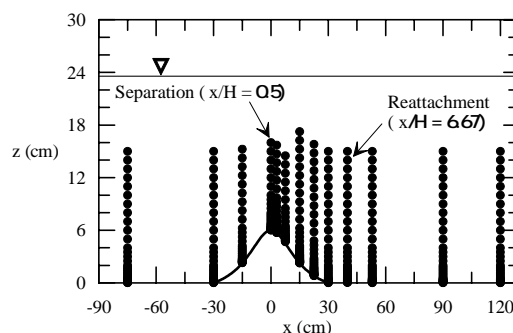
Figure 3. Description of the location of measured profiles inside the water-channel.

Undisturbed Velocity Profile

Following the approach of previous works, we will first characterize the incoming undisturbed flow.

Figure 4 shows the longitudinal mean velocity profile in physical coordinates. A power law fit to these experimental data provided an exponent of 0.15, i.e. $n = (1/6.66)$. This value, although lower than the obtained in the wind tunnel simulations (Table 5), is representative of water channel flow, following Prandtl's 1/7 power law, see Schlichting (1959).

Figure 5 presents a log-linear plot where the data is adjusted by the logarithmic law shown in Eq. 2:

$$U = \frac{u_*}{\kappa} ln\left(\frac{z}{z_0}\right)$$

(2)

where k is the von Karman constant. The values for the friction velocity, u_*, and for the roughness parameter, z_0, were obtained through the curve-fitting of the Eq. 2 to the logarithmic region of the boundary layer.
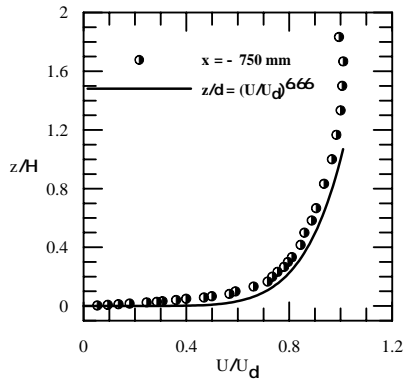

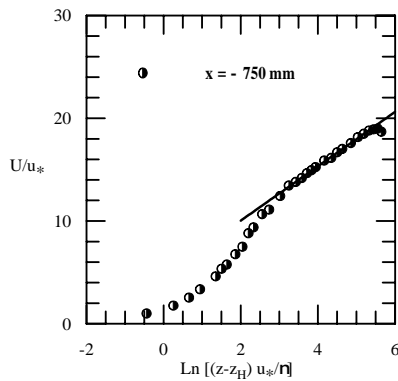**Figure 4. Longitudinal mean velocity profile, undisturbed profile.**

Figure 5. Undisturbed mean velocity profile in inner coordinates.

From the best-fit of the logarithmic law presented in Figure 5, the value of the friction velocity was calculated, giving $u_* = 0.072$ U_d This value is in 5% agreement with the data of Britter et al. (1981), $u_* = 0.0685 U_d$, and Athanassiadou and Castro (2001), $u_* = 0.06 U_d$ In fact, all the characteristic parameters of the undisturbed boundary layer are in quite good agreement with other authors, thus certifying that the simulated flow is representative of atmospheric flows. A summary of the comparison with other authors' data is presented in Table 3. The global and local properties of the undisturbed boundary layer are presented in Table 4.

	s_u / u_t	s_w / u_t
Athanassiadou and Castro (2001)	2.19	1.12
Britter et al. (1981)	2.12	-
Gong and Ibbetson (1986)	2.20	1.00
Khurshudyan (1981)	2.50	1.20
Zeman and Jensen (1983)	2.43	1.23
Present work	2.12	0.69

Table 3. Comparison of turbulent parameters with literature data.

d(mm)	U_d(m/s)	u_t (m/s)	z_0 (mm)	l (mm)	h_m (mm)
100	0.0482	0.0028	0.08	9.95	54.64

Table 4. Properties of the undisturbed boundary layer.

Mean Velocity Results

In order to identify which mechanisms are dominant in each region of the flow, the results will be split into three blocks: data for the flow field upstream of the separation point (first 3 stations), data for the recirculation region (next 7 stations) and data for the returning to equilibrium region (last 3 stations).

Longitudinal mean velocity profiles are presented in Figures 6 to 8. The flow measured on the upwind slope is shown in Figure 6, where a pronounced acceleration can be noticed on the hill top profile.

Figure 7 illustrates the velocity profiles inside the recirculation region. These profiles present characteristic mixing layer behaviour, collapsing with each other approximately on the point of maximum mean longitudinal shear gradient. Mean longitudinal velocity profiles downstream of the wake are presented in Figure 8. In this region of the flow field the boundary layer is progressively returning to its equilibrium conditions.

The separation point was observed to occur approximately at x = 30 mm, (x/H = 0.5), and reattachment was observed at around x = 400 mm, (x/H = 6.67). An overview of the recirculation region is presented in Figure 9, where the location of zero mean longitudinal velocity and the border of the separation zone are illustrated.
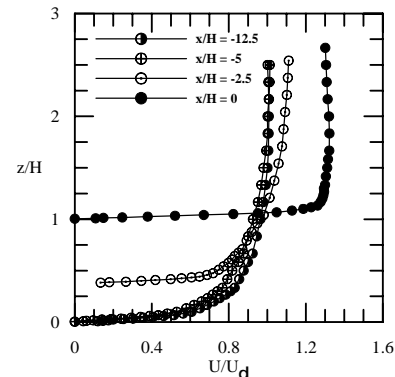

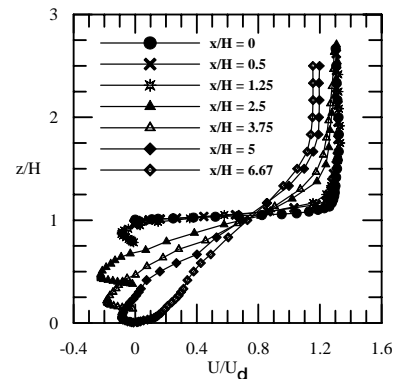**Figure 6. Longitudinal mean velocity profilesupstream and at the hill top.**

Figure 7. Longitudinal mean velocity profiles inside the recirculation region.

The mean vertical velocity profiles, W, are introduced through Figures 10 to 12. A large increase can be observed as the fluid flows

uphill, as shown in Figure 10. It is then followed by negative values of vertical mean velocity on the downside of the hill (Figure 11). In fact, due to the extension of the separation bubble that is formed, the mean z-velocity profile only becomes negative past station $x/H = 2.5$. As station $x/H = 10$ is reached, as illustrated in Figure 12, W returns to a near zero value.
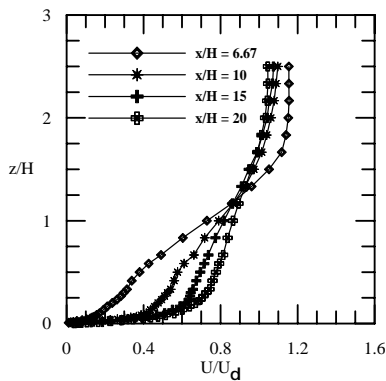

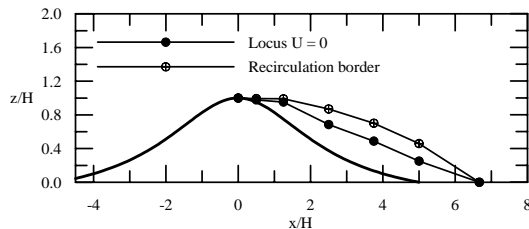**Figure 8. Longitudinal mean velocity profiles downstream of the hill.**

Figure 9. Locus of zero mean longitudinal velocity and estimated boundary for the recirculation region.
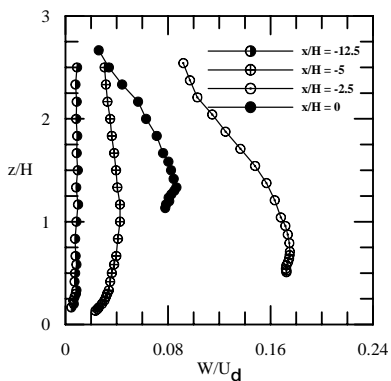
F**igure 10. Vertical mean velocity profiles upstream and at the hill top.**

Turbulent Field

The changes in Reynolds stresses are shown through Figures 13 to 21. The behaviour of the longitudinal stresses is presented in Figures 13 to 15. In Figure 13, the measurements indicate that <u'u'> recovers its maximum undisturbed value in the near-wall region at the crest of the hill. For the outer region instead, the decrease in <u'u'> with respect to its upstream value is far more pronounced. These findings are in agreement with previous field observations. In the separated flow region, illustrated in Figure 14, a substantial enhancement in <u'u'> of the order of four times, occurs.
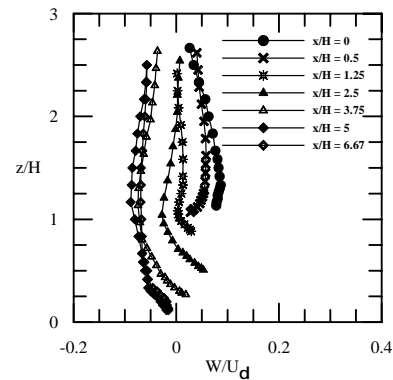
Figure 11. Vertical mean velocity profiles inside the recirculation region.
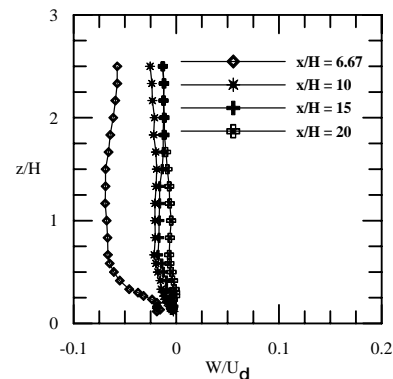
Figure 12. Vertical mean velocity profiles downstream of the hill.

The turbulence profiles inside the recirculation region are characterized by an elevated maximum whose distance to the wall increases with increasing distance from the hill. Generally, these peaks are located near the border of the recirculation zone. The peak value for <u'u'> was found for $x/H = 3.75$, near the center of the recirculation bubble. This peak is located at about $z/H = 0.8$

From Figure 15 it can be observed that the downstream profiles tend progressively to the shape of the undisturbed turbulence field, returning them to the equilibrium condition. Far away from the hill, at stations $x/H = 15$ and 20, the two <u'u'> profiles are still very distinguished between each other and different from the undisturbed profile at $x/H = -12.5$. In fact, only at station $x/H = 15$ the pronounced outer peak in <u'u'> disappears, and the inner near-wall region peak return to take place.

The changes in the vertical fluctuations are shown in Figures 16 to 18. For <w'w'> an increase of about 50 % is observed on the hill top when compared with the undisturbed values, as shown in Figure 16. This increase is followed by a further, and much more substantial, increase of about twenty fold in the separated flow region, presented in Figure 17. Indeed, we had seen previously that a large increase in W was observed uphill. The distributions of <u'u'> and of <w'w'> are somewhat similar across the separated region, although <w'w'> is about 65 % of <u'u'>. Also, we note that the maximum value of <w'w'> is found at $x/H = 3.75$, $z/H = 0.8$, just as before.

Similarly to the behaviour of <u'u'>, the marked peak in the outer region vanishes just at station $x/H = 15$. However, the inner region has not yet recovered equilibrium, as was the case for <u'u'>, since the characteristic inner layer peak (see Figure 16) is still absent. Thus, far away from the hill, at stations $x/H = 15$ and 20, the two <w'w'> profiles are still very different from each other and from the upstream behaviour.

The Reynolds shear stress measurements are shown in Figures 19 to 21. Upwind the hill, as shown in Figure 19, the Reynolds stress profile, $\langle u'w' \rangle$, is relatively small and varies slowly with height. At the hill crest, values of $\langle u'w' \rangle$ are enhanced. In the flow separated region, a large increase in $\langle u'w' \rangle$ is observed, of the order of seventeen times. The highest value of $\langle u'w' \rangle$ is achieved at location $x/H = 3.75$, $z/H = 0.6$, differently from the positions of the points of maximum for $\langle u'u' \rangle$ and for $\langle w'w' \rangle$. Between the locations of detachment and of re-attachment, an inner region of constant $\langle u'w' \rangle$ was not detected. Far downstream of the hill, at stations $x/H = 15$ and 20, $\langle u'w' \rangle$ becomes nearly constant, but assuming values almost ten times higher than its upstream values.
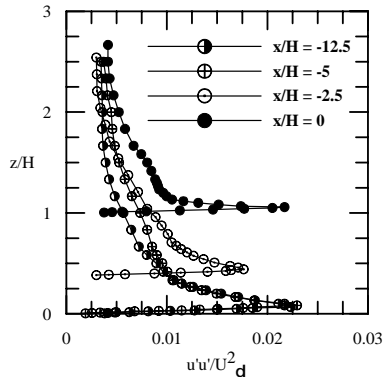
Figure 13. Longitudinal Reynolds stresses profiles upstream and at the hill top.
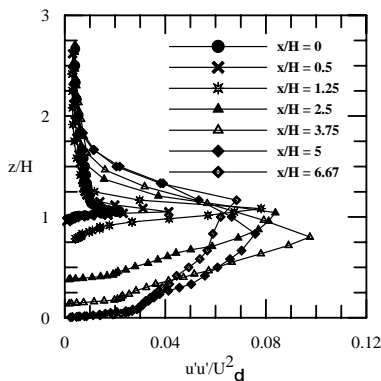
Figure 14. Longitudinal Reynolds stresses profiles inside the recirculation region.
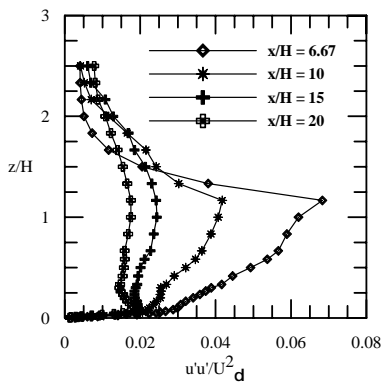
Figure 15. Longitudinal Reynolds stresses profiles downstream of the hill.
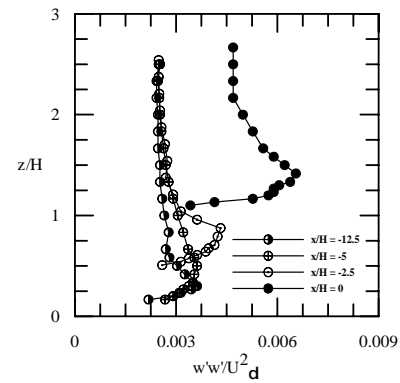
Figure 16. Vertical Reynolds stresses profilesupstream and at the hill top.
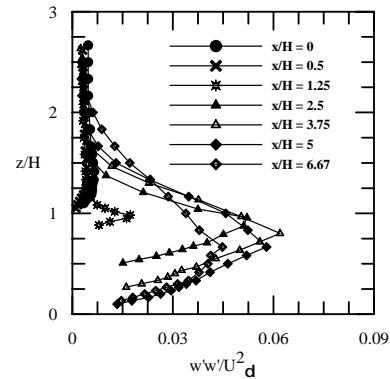
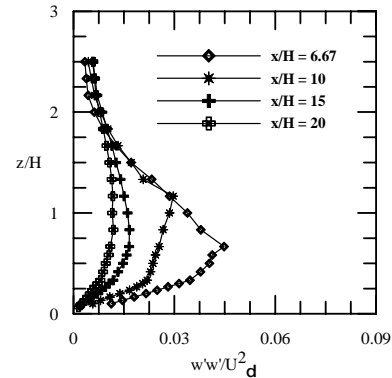**Figure 17. Vertical Reynolds stresses profiles inside the recirculation region.**

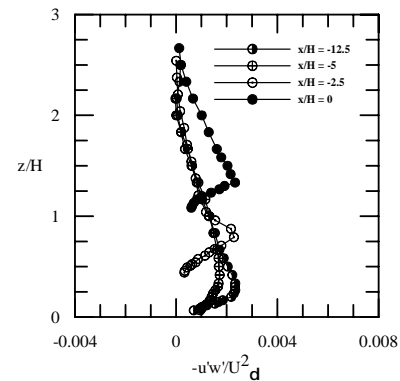**Figure 18. Vertical Reynolds stresses profiles downstream of the hill.**

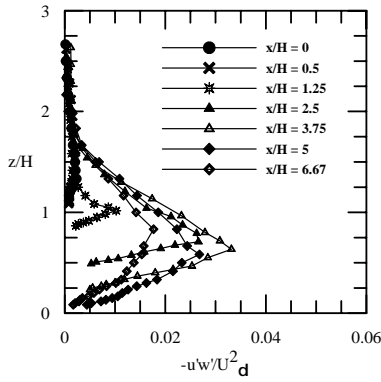**Figure 19. Reynolds shear stresses profiles upstream and at the hill top.**

Figure 20. Reynolds shear stresses profiles inside the recirculation region.
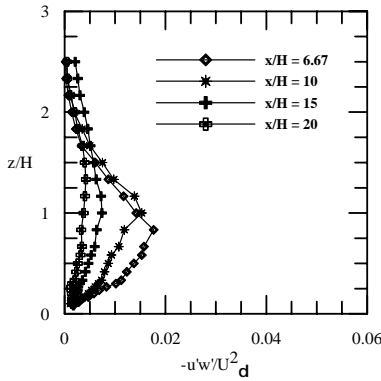

Figure 21. Reynolds shear stresses profiles downstream of the hill.

Production Terms

In order to better understand the dynamics of the turbulent field, we will now resort to the production terms of the equation of transport of the Reynolds stress terms. Considering a two-dimensional boundary layer problem, the dominant terms can be written as:

$$P_{uu} = -2\overline{u'w'}\frac{\partial U}{\partial z}, \tag{3}$$

and

$$P_{uw} = -2\overline{w'w'}\frac{\partial U}{\partial z}. \tag{4}$$

From the above presented data, the Equations 3 and 4 have been calculated. The results obtained for the production terms are shown in Figures 22 to 27.

The production terms for $\langle u'u'\rangle$ and for $\langle u'w'\rangle$ are presented in Figures 22 to 24, and Fig. 25 to 27, respectively. Through Figure 22, it can be clearly seen the behaviour predicted by the rapid distortion theory for the hilltop profile, i.e., that in the near-wall region the longitudinal turbulence levels remain approximately equal to its upstream values, whilst for the outer sublayer $\langle u'u'\rangle$ shows a significant decrease.

For the upstream and downstream attached velocity profiles, both production terms reach a maximum very close to the wall. Approaching the top of the hill, P_{uu} decreases whereas P_{uw} suffers a large increase, as depicted in Figure 25. The production term P_{uw} has an increase on top of the hill of about ten times its maximum upstream value. In fact, a difference of at least one order of

magnitude is established between the two production terms upstream at x/H = 0.

In the separated flow region, both production terms reach a maximum in the middle of the separation bubble, see Figures 23 and 26. The production term P_{uu} increases by at least one order of magnitude in the separated flow region as compared to its undisturbed upstream values. The same behaviour is observed for P_{uw} for it has a further ten times increase in the separated flow region with the peak moving away from the wall.
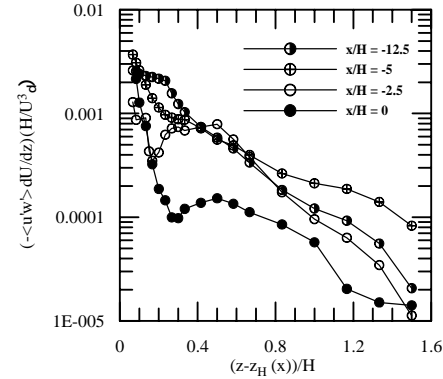

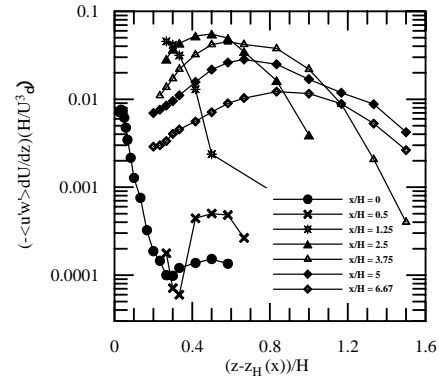**Figure 22. Production term of the longitudinal turbulent kinetic energy upstream and at the hill top.**

Figure 23. Production term of the longitudinal turbulent kinetic energy inside the recirculation region.
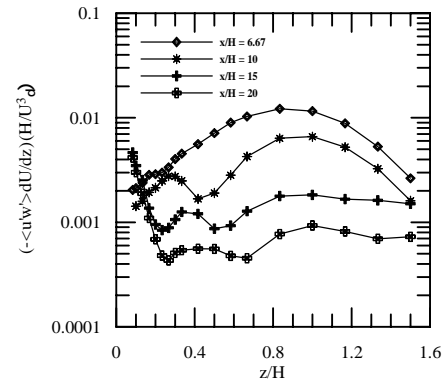

Figure 24. Production term of the longitudinal turbulent kinetic energy downstream of the hill.

The peaks in turbulence production for <u'u'>and for <u'w'> do not coincide for the present data; the peak for P_{uu} is reached at $x/H = 1.25$ whereas the peak for P_{uw} is reached at x/H = 2.5.

In the downstream region, the production terms are returned to their upstream shapes. From Figures 24 and 27 we notice the inner-layer peaks returning to take place, while the amplified production in the outer region, introduced by the separation region, is progressively decaying.
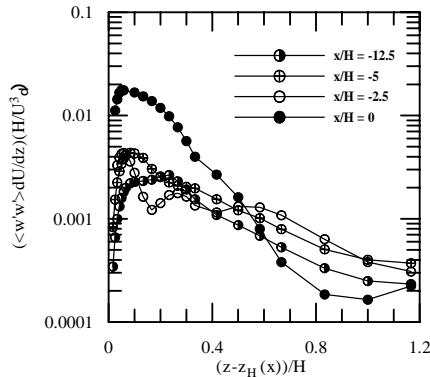

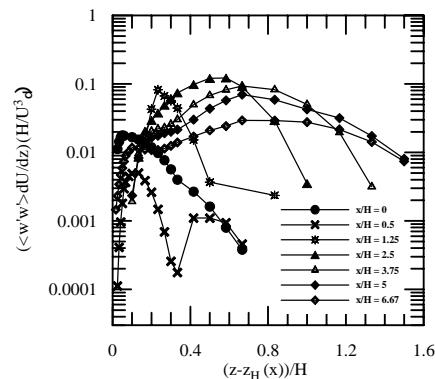**Figure 25. Production term of <u'w'> upstream and at the hill top.**

Figure 26. Production term of <u'w'> inside the recirculation region.

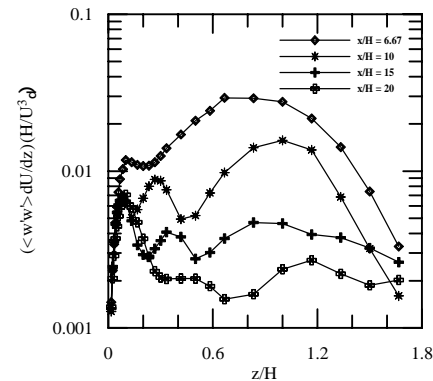**Figure 27. Production term of <u'w'> downstream of the hill.**

Skin Friction

Many existing methods that are used to measure the skin-friction rely in one way or another on the hypothesis that in the boundary layer the mean velocity profile assumes a logarithmic form at a certain distance from the wall. In fact, chart methods based on the existence of a logarithmic velocity profile have become so much popular that some classifications of the available techniques

frequently separate them into techniques that comply to the conditions set by the classical law of the wall and those that do not. The Preston tube and the Clauser-chart method are, of course, strongly dependent on the log-law assumption.

In a separated flow region, the near wall flow will not follow a logarithmic profile. Other techniques should be used to measure the skin-friction: direct methods, analogies or liquid tracers. In our problem geometry, the curved surface prevents the use of direct method in general. Thus, it appears that, with the type of flow to be studied here, the only feasible way to find the skin-friction is through a detailed analysis of the velocity profiles in the viscous wall region.

In a turbulent boundary layer, the very near wall region is dominated by viscous effects. Under pressure gradient conditions, the viscous sub-layer equation relates the viscosity and pressure terms solely. A double integration of this equation furnishes a parabolic relationship between the velocity and the distance from the wall. Thus, provided detailed measurements are made in the viscous region, this procedure can be used to find not only u_* but also the longitudinal pressure variation. In principle, this approach should be valid in the whole flow region giving us a method to find the friction velocity even in the flow separated region.

In the attached flow region, in places where the logarithmic velocity profile is valid, it can then be discriminated through Equation 2.

In a third procedure, consider the Reynolds shear stress, <u'w'>, to be the dominant part of the shear stress outside the viscous layer. Then assuming that its vertical variations are negligible, we have $<u'w'> = u_*^2$.

For flows over a flat wall, the x-coordinate can be aligned with the mean flow direction, resulting in a rectangular Cartesian system where the momentum balance in x-direction contains most of the dynamical information regarding the flow.

For flows over curved surfaces, however, identifying a coordinate system where the main coordinate axis is aligned with the flow direction is a problem. To overcome this difficulty, Finnigan (1983) suggests the use of physical streamlined coordinates. These coordinates are, however, difficult to use in separated flow regions. Thus, most of the data presented in literature for flows over hills follow a rectangular Cartesian system, just as we have presented our data in the previous section.

In our problem, the near wall measurements that are to be considered for evaluation of the skin-friction in the flow separated region, were made for distances smaller than 3 mm from the wall. In fact, in the first 3 mm, eight points are to be considered for flow characterization. In our worst case scenario, the wall tangent corresponds to an angle of about 14° (station $x/H = 1.25$). Since Sin 14° = 0.24, the corresponding streamwise velocity displacement along the normal direction will occur over a maximum distance of 0.7 mm. This fact, allied to the fact that $U >> W$, means that close to the wall skin-friction can be calculated directly from the procedure above stated with the rectangular Cartesian system shown in the previous section.
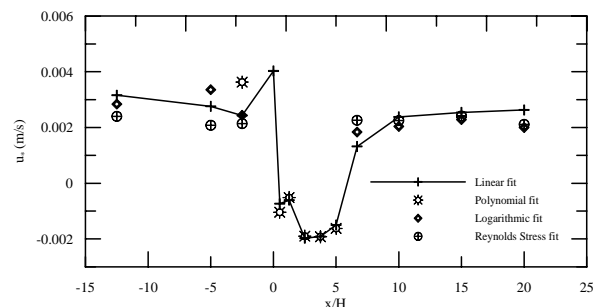

Figure 28. Global behaviour of the friction velocity along the hill.

The results obtained through four different curve fitting, i. e. a linear, polynomial, logarithmic and Reynolds stress fit are summarized in Figure 28. Further details concerning these calculations will be given in a future publication.

Wind-tunnel Experiments

Description of Apparatus and of Instrumentation

The first part of this experimental investigation was carried out in the high turbulence, low speed, open-circuit wind tunnel sited at the Laboratory of Turbulence Mechanics of the Mechanical Engineering Program (PEM/COPPE/UFRJ).

Figure 29. General of the wind tunnel.

A general view of the wind tunnel is presented in Figure 29. The test section has an overall length of 10 m, and a cross section area of 0.67 m x 0.67 m. The potential flow velocity can be made to vary from zero to 3.5 m/s with free stream turbulence intensity levels of about 2 %.

Figure 30. Stratification section of the wind-tunnel.

In still air conditions, the floor temperature can be raised up to 100 °C over a 6 m long surface. The heating system is comprised by a series of 6 one-meter long independent panels and one stratification section. Each panel is fitted with electrical resistances that furnish a wall temperature controlled variation of 2 °C, and a heating capacity of 0.75 kW/m^2. Ten horizontal resistance stripes allow the stratification section to differentially heat the incoming flow. An illustration of the stratification section is presented in Figure 30. The whole facility is capable of developing boundary

layer gradients of up 60 °C at uniform mean speeds in the range of 1.5-3.5 m/s, and the total heating capacity is of about 10 kW/m^2.

The adjustable ceiling of the wind tunnel allowed the longitudinal pressure gradient to be set nearly to zero. The vortice generators developed by Barbosa et al. (2000) have been used in order to provide thick simulated boundary layers.

Simultaneous measurement of the velocity and the temperature fields was conducted with the aid of thermal anemometry. Longitudinal mean velocity profiles and turbulence intensity levels were measured together with mean and fluctuating temperatures through a two-wire probe type Dantec 55P76. Each sensor of the probe was connected to one anemometer. The hot-wire was controlled by a constant temperature anemometer Dantec model 55M01/M10; and the cold-wire, responsible for the temperature measurements, was connected to a constant current anemometer model 56C20. A Pitot tube, a reference thermocouple, a reference electronic manometer, and a computer controlled traverse gear were also used. In getting the data, 10,000 samples were considered for the calculation of the ensemble average. An uncertainty analysis of the data was performed according to the procedure described in Kline (1985). Typically the uncertainty associated with the velocity and temperature measurements were: U = 0.0391 m/s precision, 0 bias (P=0.95); T = 0.0058 °C precision, 0 bias (P=0.99).

To obtain accurate measurements, the mean and fluctuating components of the analogical signals given by the anemometers were band-pass filtered, then amplified with a gain controlled between 1 and 500 and shifted by an offset so as to adjust the amplitude of the signal to the range of the 16-bit A/N converter. The hot-wire and the cold-wire were calibrated in the thermal wind tunnel. The calibration procedure made use of a system where the velocity and the temperature of the income flow could be controlled independently. Further details can be found in Loureiro et al. (2001).

In order to estimate the onset and extent of the separated region, a flow visualisation study was performed.

Two hills of the same geometry and proportions have been done for the present study. For the wind-tunnel experiments, owing to the interest in studying stratified flows, the hill was made of aluminum and equipped with an individual heating system. Inside the hill, electrical resistances were fitted so that each slope could be heated independently. The knob of the thermostat was regulated in each run to provide a uniform surface heating in agreement with the wind tunnel floor temperature.

Figure 31. Model of the hill inside the wind tunnel.

Stability Considerations

The flow of a fluid over surfaces that present large changes in elevation is controlled by the large-scale changes in the pressure field. The internal gravity waves generated by the hills are the key effect on the definition of the drag that will be exerted over the atmospheric boundary layer.

In statically stable conditions, the vertical oscillations of air parcels take on the Brunt-Väisälä frequency, Eq 5:

$$N = \left(\frac{g}{\overline{\theta}} \frac{\partial \overline{\theta}}{\partial z} \right)^{1/2}. \tag{5}$$

When oscillating air parcels are transported downwind at a mean speed, U, a wave is traced by the parcels. Taking as a characteristic length of the hill its half-width at half-width height, L_H, the time an air parcel takes to traverse the hill is L_H/U. We define the Froude number as the ratio of the time during which an air parcel is displaced vertically to the time an air parcel takes to traverse the hill, Eq. 6:

$$F_L = \frac{U}{NL_h}. \tag{6}$$

A variety of flows are possible depending on the value of Froude number. For the neutral case, strong winds and neutral stability, N approaches zero so that F_h approaches infinity. In this situation, the oncoming streamlines are deflected upwind and above the will to a distance of about three times the height of the hill. At the top of the hill the streamlines are brought together causing a speed up of the wind. A short review of neutral stability flows was presented by Loureiro et al. (2000a, 2000b). For further details on the neutral flows the reader is referred to these publications.

Under diabatic conditions, the effects of stability can be classified according to $F_L = U/(NL_h)$ and $F_h = U/(Nh)$. There are six classification classes in total, which can be found in Kaimal and Finnigan (1994) or in Loureiro et al. (2001).

Another important parameter for the classification of the atmospheric stability is the Monin-Obukhov length. It is usually recognised by meteorologists to be the appropriate parameter to measure stability in the surface layer; it is given by Eq. 7:

$$L = -\frac{u_\tau^3}{\chi \left(g/\overline{\theta} \right) \overline{\left(w'\theta' \right)}_0}, \tag{7}$$

where u_τ denotes the friction velocity, κ, the von Karman constant and $\overline{\left(w'\theta' \right)}_0$ the temperature flux at the wall.

An alternative classification of the level of atmosphere instability is through the Richardson number. Since it can be easily evaluated from one temperature profile, this parameter is widely used in laboratory simulations of the atmospheric boundary layer. The bulk Richardson number can be evaluated according to Eq. 8:

$$Ri_b = \frac{gH}{\overline{T}} \frac{\left(T_H - T_0 \right)}{U_H^2}, \tag{8}$$

where the subscripts H and 0 indicate the position in which the measurements are taken: H indicates the higher position of the probe, 0 indicates the lower position.

A normal practice in literature is to divide the boundary layer into two portions and evaluate the Richardson number in both of them.

Results for The Velocity and The Temperature Fields

This subsection presents the results for the stratified boundary layers over a steep hill simulated in the atmospheric wind-tunnel. Measurements were performed for three stations: at the upstream base, x = - 300 mm, at the hill crest, x = 0 mm and downstream of the recirculation region, x = 530 mm. Due to the geometry of the hot-wire probe chosen for this work and the curvature of the hill, it was not possible to investigate the near-wall flow along the slopes of the model. However, new arrangements using different probe types and probes support are currently being tested, suggesting that better spatial resolution will be achieved for future work.

Please note that the origin of the coordinate system is located on the symmetrical axis of the hill, at ground floor level. This is illustrated in Figure 32. The free-stream velocity was set equal to 2.01 m/s during this set of experiments, and it was kept constant by monitoring the response of an electronic pressure transducer connected to a Pitot tube inside the test section. The velocity on the outer edge of the boundary layer, U_d, was calculated as 0.98 of the free-stream velocity. The parameter used for normalization of all velocity profiles was based on the incoming flow under neutral conditions, $U_d = 1.97$ m/s.

As will be explained in the next section, the recirculation region extended from 30 mm to 400 mm. It must be stated here that the last station investigated, at x = 530 mm, was completely outside the separation zone, and therefore all the data acquired through thermal anemometry do represent the actual flow with a high confidence level.
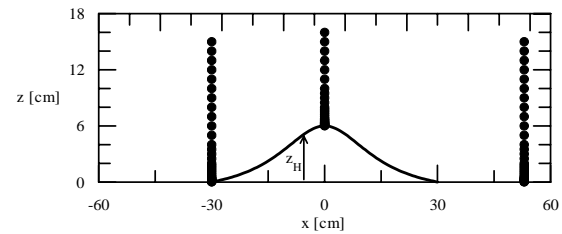

Figure 32. Illustration of the coordinate system and measured profiles.

The standard approach to the study of flow over hills is based on the concept of perturbation techniques. Therefore, the flow over the hill (U) is treated as the incoming undisturbed flow, (U_0) plus a perturbation ΔU, introduced by the presence of the hill, i.e. $U = U_0 + \Delta U$.

Hence, before we proceed to the effects of the hill over the flow, let us first evaluate the effect of the stratification on the oncoming undisturbed flow. The flow global properties measured at station x = - 30 cm are shown in Table 5. This Table shows that under the effects of stratification the velocity profile becomes more "full" suffering a considerable decrease in the momentum thickness parameter. This increase in velocity in the lower portions of the flow will eventually result in an increase in the speedup factor. In Table 2, G represents the Clauser factor, u_* is the friction velocity, s_u/U_d is the ratio between the fluctuating velocity, $\langle u'^2 \rangle^{0.5}$, and the velocity at the outer edge of the boundary layer, d is the boundary layer thickness, d_2 is the momentum thickness and n is the power law exponent.

	Stable Boundary Layer	Neutral Boundary Layer	Unstable Boundary Layer
G	7.12	8.48	7.40
u_* (m/s)	0.082	0.079	0.081
s_u/U_d	2.51	2.30	3.39
d (m)	0.108	0.120	0.146
d_2 (m)	0.012	0.018	0.014
n	0.21	0.27	0.20

Table 5. Global properties of the boundary layers.

Thus, we have reached the main objective of the present work: to investigate the conditions in which the location and intensity of the maximum wind speed vary with upstream stratification. In particular, does the shape of the hill have the same effect in neutral and in stratified conditions?

This question arises in practical situations related to air pollution dispersion, the estimation of wind loads and the siting of wind turbines. The paper of Hunt et al. (1988a) addressed theoretical considerations on the problem for flow over low hills. Here we will characterise the flow over steep hills.

Neutral Atmosphere

The structure of the neutral boundary layer is shown in Figures 33 to 35. Hereafter, the velocity profiles are normalised by the free-stream velocity of the incoming profile, U_d = 1.97 m/s, and the distance from the wall is made nondimensional by the hill height, H. When the results for the evaluation of the logarithmic region are presented, the skin-friction velocity of the undisturbed profile, u_*, is used as the scale parameter.

The mean velocity profiles upstream of the hill are shown to satisfy the law of the wall and the law of the wake. When plotted in linear co-ordinates, the boundary layer followed a power law with an exponent n = 0.21, which characterizes a typical flow of a rural type boundary layer.

The downstream profile presented in Figure 34, although perturbed by the presence of the recirculation region, is also observed to follow a logarithmic behaviour. On the other hand, at the hill top, the behaviour of the velocity profile clearly do not satisfy the classical log-law.

Turbulent velocity fluctuations are presented in Figure 35. It can be noticed that the undisturbed flow follows the classical behaviour of the longitudinal turbulence intensity profile. At the hill top the intensity of these fluctuations are suppressed, as a consequence of the rapid distortion theory.
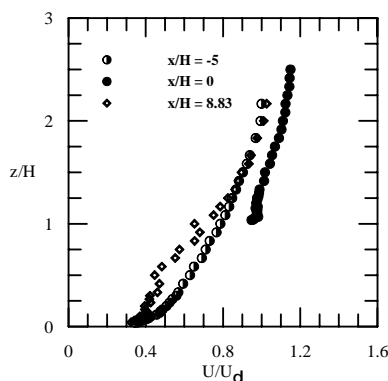

Figure 33. Mean velocity profiles in physical coordinates. Neutral boundary layer.
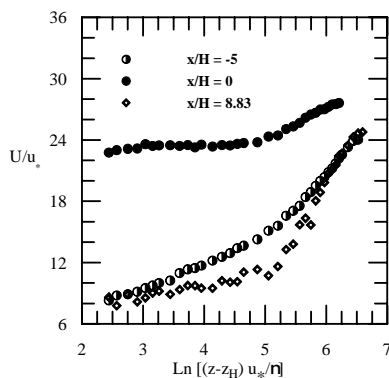

Figure 34. Mean velocity profiles in inner coordinates. Neutral boundary layer.
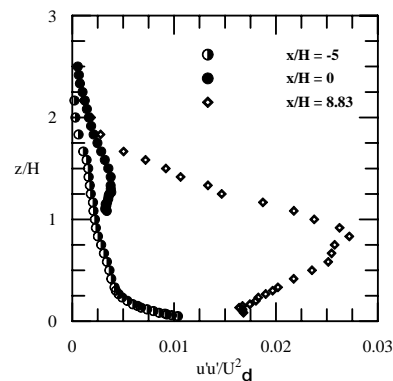

Figure 35. Longitudinal Reynolds stress profiles. Neutral boundary layer.

As above stated, the last measured station was highly influenced by the recirculation region. This can be observed in Figures 34 and 35. The leeward turbulent fluctuation profile presents a quite distinct behaviour, with its peak moving from the near-wall region outwards into the boundary layer. The high turbulence levels observed at this station is a direct consequence of the intense mixing present inside the recirculation region.

Stable Atmosphere

The behaviour of the stable boundary layer is shown in Figures 36 trough 41. From Figure 36, it can be noticed that the momentum thickness is indeed less than the one for neutral atmosphere. This picture shows, in addition, that the stability of the atmosphere has led to an increase in the velocity magnitude on the top of the hill, especially in the outer region of the boundary layer.

Results also indicate that the stability condition has contributed to an inhibition of the recirculation region. This conclusion can be reached by comparing the extension of the region of dispersed points downstream of the hill (Figures 36 and 37) with the neutral condition (Figures 33 and 34).

Figure 38 shows as well a slight decrease in the turbulence levels at the leeward side, and a small increase in the turbulence levels at the hill crest with respect to the neutral case.

Figure 39 shows that for most of the boundary layer there exists a positive temperature gradient across it. This simulated boundary layer is stably stratified with a relatively weak stratification of about 21 Km^{-1} in the lowest 50 mm, and with a much stronger stratification of about 100 Km^{-1} above. As previously discussed, the stable stratification is often discussed in terms of the Brunt-Väisälä frequency, N. For the present case, N is of about 0.85 s^{-1} in the inner sublayer, and 1.85 s^{-1} for the outer region.

The temperature data plotted in inner coordinates are shown in Figure 40. Although the three measured profiles present a good self-similarity, the classical law of the wall behaviour is not verified for the temperature field along the entire hill.

Temperature fluctuations are presented in Figure 41. The location of the peaks of the fluctuation profiles are observed to occur approximately when the mean temperature gradients achieve its maximum value. This characterizes the physical behaviour of the stable boundary layer, i.e. the fluctuations achieve a higher value exactly when the two parcels of fluid with different temperature, or density distributions, are interacting and thus forming a thin mixing layer. On the hill top, a slight decrease in temperature fluctuation can be observed. As for the near-wall region, the downstream profile presented the highest fluctuations.

Unstable Atmosphere

Results for the unstable boundary layer are presented in Figures 42 to 47. Figure 42 shows that the momentum thickness is once

more lower than the neutral case. The unstable condition, due to intensified mixing process, has promoted a faster recovery for the downstream profile. The hill top acceleration is approximately equal to the results obtained for the stable configuration. However, there is an inversion on the near-wall region on the top. This is a direct influence of the temperature field.

Figure 43 shows that the oncoming flow has maintained the classical logarithmic behaviour. However, the law of the wall and the law of the wake for the velocity field show marked departures from the stable flow case.

Considering the dispersed points in Figures 42 and 43 we can estimate that the recirculation region under unstable condition had an intermediate size between the neutral case, which had the longer recirculation zone, and the stable case, that inhibited separation.

Figure 45 shows that across the boundary layer there exists a strong negative temperature gradient, so that the flow is unstable. Using the bulk Richardson number given in Eq. 8, it was found that for the inner region Ri = -0.015, which classifies the simulated boundary layer as moderately unstable. Indeed, as commented in first section, a huge amount of surface heat flux is needed to achieve some extreme instability conditions that take place in the atmosphere.

The law of the wall for the temperature field that virtually did not exist for the stable case can be clearly seen in the far downstream station (x = 530 mm), Figure 46.
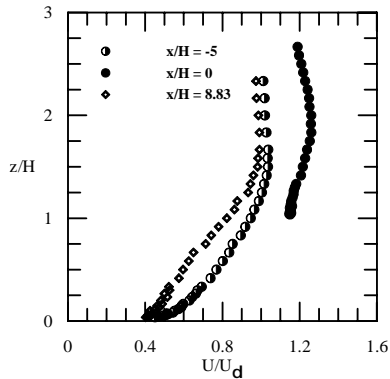

Figure 36. Mean velocity profiles in physical coordinates. Stable boundary layer.
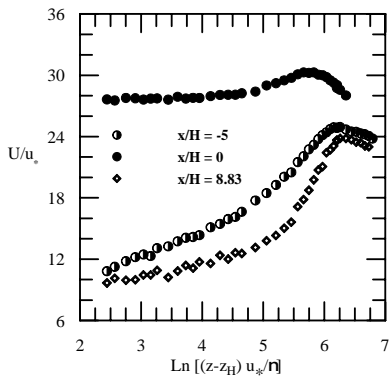

Figure 37. Mean velocity profiles in inner coordinates. Stable boundary layer.
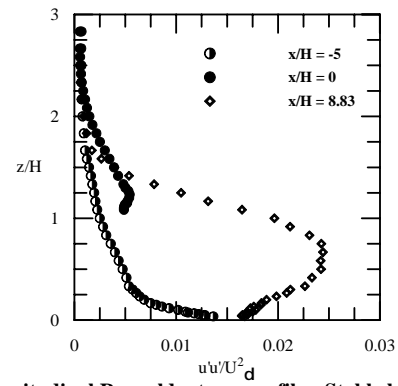

Figure 38. Longitudinal Reynolds stress profiles. Stable boundary layer.

Figure 47 shows the temperature fluctuations for the unstable condition. A sharp difference between the behaviour of fluctuations for the stable and unstable conditions can be observed. Actually, the mechanisms involved in these two situations are quite distinct. The thin mixing layer present between the lower cooler air stream and the upper warmer sublayer in the stable condition is no longer present. Instead, a widespread bigger mixing layer is formed under the unstable stratification condition. Consequently, as depicted in Figure 47, the highest temperature fluctuations are located in the near wall region.

The effects of stratification on the velocity flow will be illustrated through the speed up factor and the heat up/down factor, which can be defined as:

$$\Delta S = \frac{U(x,z) - U_0(z)}{U_0(z)}, \tag{9}$$

and

$$\Delta T = \frac{T(x,z) - T_0(z)}{T_0(z)}, \tag{10}$$

where the subscript stands for undisturbed upstream reference conditions.

Values of the speed up and the heat up/down coefficients are shown in Figures 48 and 49.
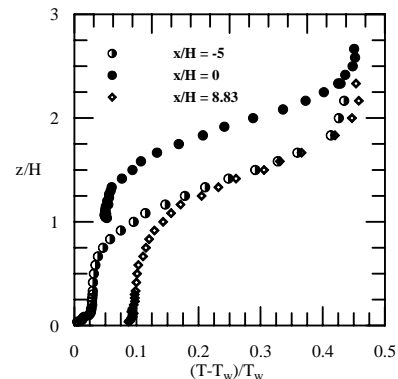

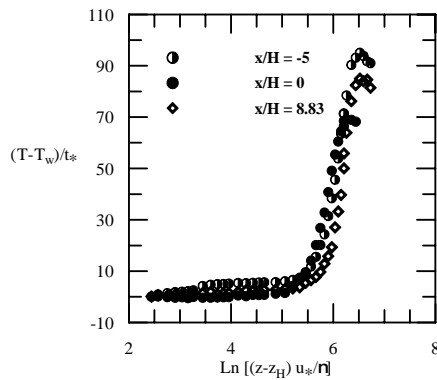**Figure 39. Mean temperature profiles in physical coordinates. Stable boundary layer.**

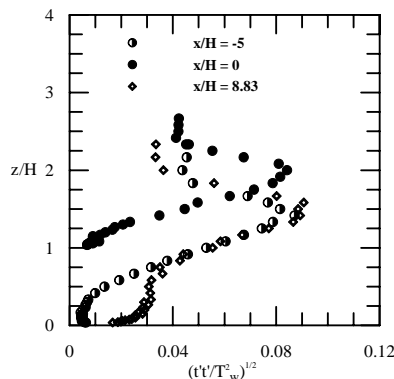**Figure 40. Mean temperature profiles in inner coordinates. Stable boundary layer.**

Figure 41. Temperature fluctuating profiles in inner coordinates. Stable boundary layer.

Figure 43. Mean velocity profiles in inner coordinates. Unstable boundary layer.

Figure 44. Longitudinal Reynolds stress profiles. Unstable boundary layer.

According to the measurements, Δs was found to vary between 2.0 and 0.24 from wall to mean stream position. These values are always higher than those obtained through Hunt et al. (1988b)'s formulation. For the neutral case, for example, The theory of Hunt et al. (1988b) gives for the height of the intermediate region $h_m = 0.10$ m, the inner sublayer thickness as $l = 0.019$ m and $\Delta s_{max} = 0.12$ at $l/3 = 0.0063$ m. However, from the experiments, we have $h_m = 0.0546$ m, $l = 0.010$ m and $\Delta s_{max} = 1.5$ at $l/3 = 0.003$ m.
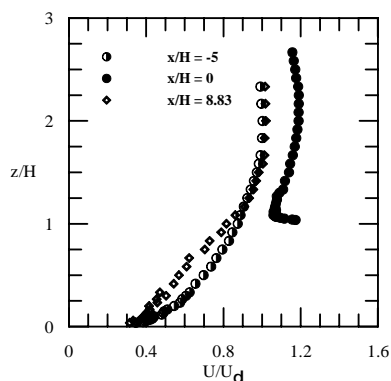

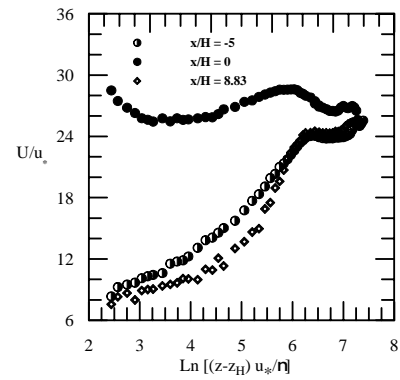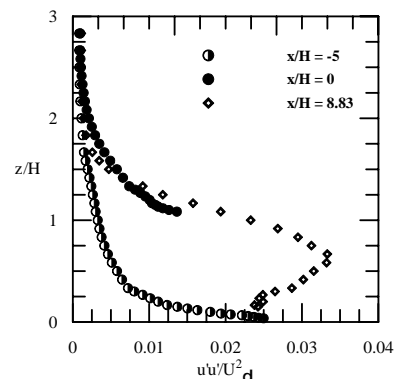**Figure 42. Mean velocity profiles in physical coordinates. Unstable boundary layer.**

Since the formulation of Hunt et al. (1988b) was developed for flows over hills of low slopes, it is no surprise to find this theory fails for the present conditions, where the nonlinear effects introduced by the separation region is believed to play an important role in the whole phenomenon.

The evidence given by Figure 48 is that under stable conditions the speed up factor decreases whereas under unstable conditions it increases.

The heat up/down factor is shown in Figure 49, which indicates that for stable flows it is mostly positive whereas for unstable flow it is mostly negative.

For flows over low hills, Hunt et al. (1988a) have shown that under weak stratification, stable or unstable, the turbulence and the velocity profile in the middle region are affected.
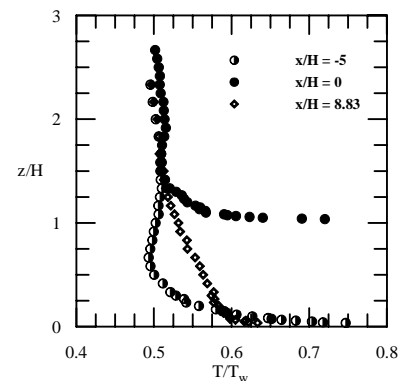

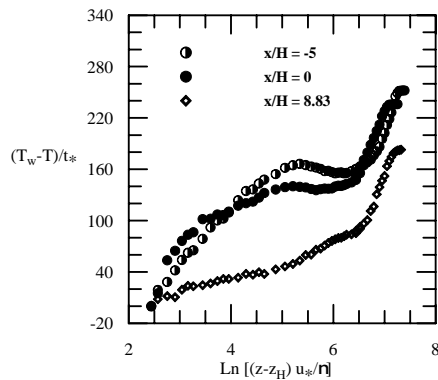**Figure 45. Mean temperature profiles in physical coordinates. Unstable boundary layer.**

Figure 46. Mean temperature profiles in inner coordinates. Unstable boundary layer.
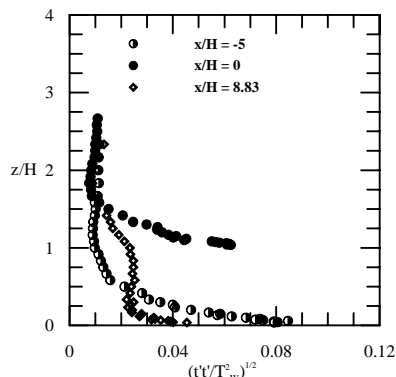

Figure 47. Temperature fluctuating profiles in inner coordinates. Unstable boundary layer.

The stratification, however, is too weak to affect the dynamics of the flow over the hill. When the temperature gradient in the approaching flow is large enough to characterize a moderate stratification, then the buoyancy forces greatly affect the mean flow provoking changes in the speed up factor of up to 20%. These trends were mostly observed for stable conditions with the streamlines approaching the surface of the lee slopes. In unstable conditions, the authors claim that no major change in the pattern of the perturbation flow would occur.

As illustrated by Figures 48 and 49, we have found very different results for the present experimental conditions. Both flow patterns for stable and unstable conditions clearly suffered large changes due to stratification.
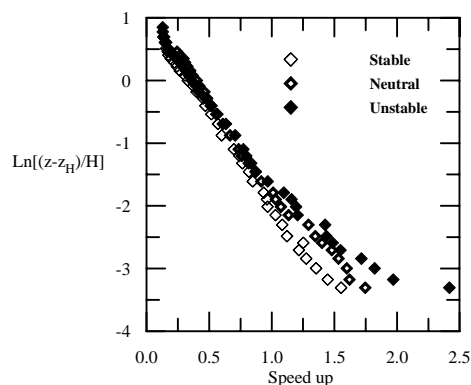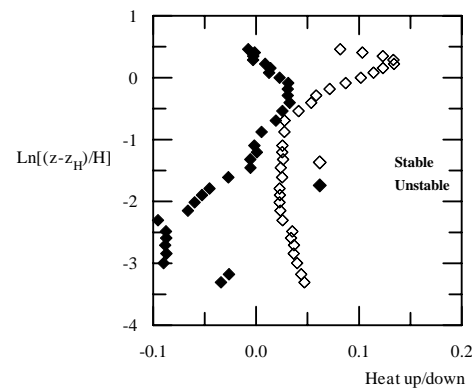

Figure 48. Speed-up factor.

Figure 49. Heat up/down factor.

Final Remarks

The present work has investigated the effects that a large change in surface elevation provokes on the properties of the atmospheric boundary layer. In particular this investigation has focused on two main aims: (i) to characterize the influence exerted by the leeside separation region on the properties of the whole flow field, and (ii). to study the behaviour of stratified boundary layer subjected to an abrupt change in surface elevation.

Regarding the effects of the recirculation region of the flow field, water-channel simulations of a neutrally stratified boundary layer have been performed. Measurements of mean longitudinal and vertical components, along with the Reynolds stress terms have been conducted through laser-Doppler anemometry. In particular, detailed near-wall data have been acquired inside the separated region. Mean velocity results were compared the predictions of the linear theory of Jackson and Hunt (1975). The turbulent flow field was analysed on the basis of the local equilibrium concept and the rapid distortion theory, introduced by Batchelor and Proudman (1954) and described by Townsend (1976).

Results for the turbulent intensities have shown that $\langle u'u'\rangle$ recovers its maximum undisturbed value in the near-wall region at the crest of the hill. For the outer region instead, the decrease in $\langle u'u'\rangle$ with respect to its upstream value is far more pronounced. For $\langle w'w'\rangle$ an increase of about 50 % is observed on the hill top when compared with the undisturbed values. This increase is followed by a further, and much more substantial, increase of about twenty fold in the separated flow region. These findings are in agreement with previous observations of Bradley (1980) and Zeman and Jensen (1987), and in accordance with the rapid distortion theory predictions.

Owing to the thorough description of the inner region provided by these measurements, linear, parabolic and logarithmic fits have been adjusted to the data, providing calculations for the skin friction velocity. In addition, u* have also been calculated through the Reynolds shear stress profiles, allowing four different ways of finding the friction velocity.

To fulfill the latter objective, mean velocity and temperature profile measurements were made with the aid of thermal anemometry, in a wind tunnel environment. Results were presented with particular emphasis on the behaviour of the speed up factor and the heat up/down factor. It was found that the stable conditions provoked a decrease in speed up factor whereas the unstable conditions provoked an increase. The findings were compared with theory of Hunt et al. (1988a,b) providing poor agreement; they, however, have shown that turbulent transfer has a strong influence on the near wall scalar fields and vice-versa. In fact, since Hunt's theory was devised for hills of low slopes, the experimental results were not expected to collapse with the theoretical predictions.

The mean velocity profiles measured through hot-wire anemometry indicate that the changes in stratification did also influence the extension of the recirculation region and, consequently, its effects on the mean flow field. Future investigations intend to quantify these changes through laser-Doppler anemometry.

Difficulties in modelling some important flow characteristics, e. g. the speed-up factor and the drag caused by the elevation, and how do these quantities vary under different stratification conditions, have lead to significant forecasting errors. The present work has striven to contribute to a better understanding of the problem by generating an extensive and detailed experimental research on the topic.

Hence, this dataset constitutes a good test to evaluate the capability of numerical weather forecast models in predicting the true behaviour of the flow field under adverse conditions.

Acknowledgments

References

Arya, S. P. S., Capuano, M. E. and Fagen, L. C.; "Some Fluid Modelling Studies of Flow and Dispersion Over Two-Dimensional Low Hills", Atmospheric Environment, vol. 21, 753-764, 1987.

Arya, S. P. S. and Gadiyaram, P. S.; "An Experimental Study of Flow and Dispersion in the Wakes of trhee-dimensional Low Hills", Atmosph. Environment, vol. 20, 729-740, 1986.

Athanassiadou, M. and Castro, I. P., "Neutral Flow Over a Series of Rough Hills: A Laboratory Experiment", Boundary-Layer Meteorology, vol. 101, 1-30, 2001.

Barbosa, P. H., Cataldi, M. and Silva Freire, A. P., "Wind tunnel simulation of atmospheric boundary layers", Journal of the Brazilian Society of Mechanical Engineering, vol. 24, 3, 177-185, 2002.

Batchelor, G. K. and Proudman, I.; "The Effect of Rapid Distortion on a Fluid in Turbulent Motion", Quart. J. Mech. Appl. Math., vol. 7, 83-103, 1954.

Belcher, S. E. and Hunt, J. C. R.; "Turbulent Flow over Hills and Waves", Annu. Rev. Fluid Mech., vol. 30, 507-538, 1998.

Bowen, A. J.; "The Prediction of Mean Wind Speeds Above Simple 2D Hill Shapes", J. Wind Eng. Ind. Aerodynamics, vol. 15, 259-270, 1983.

Bradley, E. F.; "An Experimental Study of The Profiles of Wind Speed, Shearing Stress and Turbulent Intensities at The Crest of a Large Hill", Q. J. R. Meteorological Society, vol. 106, 101-124, 1980.

Britter, R. E., Hunt, J. C. R. and Richards, K. J.; "Airflow Over a Two-dimensional Hill: Studies of Velocity Speedup, Roughness Effects and Turbulence", Q. J. R. Meteorological Society, vol. 107, 91-10, 1981.

Carruthers, D. J. and Choularton, T. W.; "Airflow Over Hills of Moderate Solpe", Q. J. R. Meteorological Society, vol. 108, 603-624, 1982.

Carruthers, D. J. and Hunt, J. C. R.; "Fluid Mechanics of Airflow over Hills: Turbulence, Fluxes and Waves in The Boundary Layer", Atmospheric Processes Over Complex Terrain, Chapter 5, 83-103, American Meteorological Society, 1990.

Castro, I. P. and Snyder, W. H.; "A Wind-tunnel Study of Dispersion From Sources Downwind of Three-dimensional Hills", Atmosph. Environment, vol. 16, 1869-1887, 1982.

Finnigan, J. J., "A streamlined coordinate system for distorted turbulent shear flows", J. Fluid Mechanics, vol. 130, 241-258, 1983.

Gyure, B. and Janosi, I. M.; "Stratified Flow Over Asymmetric and Double Bell-shaped Obstacles", Dynamics of Atmospheres and Oceans, vol. 37, 155-170, 2003.

Jackson, P. S. and Hunt, J. C. R.; "Turbulent Wind Flow Over a Low Hill", Q. J. R. Meteorological Society, vol. 101, 929-955, 1975.

Hunt, J. C. R., Richards, K. J. and Brighton, P. W. M.; "Stably stratified shear flow over low hills", Q. J. R. Met. Soc., vol. 114, 859-886, 1988a.

Hunt, J. C. R., Leibovich, S. and Richards, K. J.; "Turbulent Shear Flow Over Low Hills", Q. J. R. Met. Soc., vol. 114, 1435-1470, 1988b.

Kaimal, J. C. and Finnigan, J. J.; "Atmospheric Boundary Layer Flows, Their Structure and Measurement"; Oxford University Press, 1994.

Kline, S. J., "The Purpose of Uncertainty Analysis", J. Fluids Engineering, 107, 153-160, 1985.

Lamb, V. R. and Britter, R. E.; "Shallow flow over an isolated obstacle", J. Fluid Mechanics, 147, 291-313, 1984.

Long, R. R.; "The Motion of Fluids with Density Stratification", J. Geophysical Research, vol. 64, 2151-2163, 1959.

Loureiro, J. B. R., Vasques, F. S., Rodrigues, D. A., Terra, R. J. and Silva Freire, A. P.; "A wind tunnel study of turbulent flow over hills. Part I: Smooth changes in surface elevation", VII National Congress of Thermal Sciences (ENCIT) , Porto Alegre, October, 2000a.

Loureiro, J. B. R., Vasques, F. S., Rodrigues, D. A., Terra, R. J. and Silva Freire, A. P.; "A wind tunnel study of turbulent flow over hills. Part II: Large changes in surface elevation", VII National Congress of Thermal Sciences (ENCIT) , Porto Alegre, October, 2000b.

Loureiro, J. B. R., Cataldi, M. and Silva Freire, A. P.; "An experimental study of turbulent stratified flows over hills with large changes in surface elevation", XVI Brazilian Congress of Mechanical Engineering (COBEM), Uberlândia, December, 2001.

Meroney, R. N.; "Fluid Dynamics of Flow Over Hills/Mountains - Insights Obtained Through Physical Moddeling", In: Atmospheric Processes Over Complex Terrain, Chapter 7, 145-171, American Met. Soc., 1990.

Meroney, R. N. and Cermak, J. E.; "Modeling of atmospheric transport and fumigation at shoreline sites", Boundary-layer Met., 9., 1975.

Ogawa, Y., Diosey, P. G., Uehara, K., and Ueda, H; 'Wind tunnel observation of flow in diffusion under stable stratification", Atmospheric Environment, vol. 19, 65-74, 1985.

Ohba, R., Ukegushi, N., Kakishima, S and Lamb, B.; "Wind tunnel experiment of gas diffusion in stably stratified flow over a complex terrain", Atmospheric Environment, 24A, 1987-2001, 1990.

Ohba, R., Hara, T., Nakamura, S., Ohya, Y. and Uchida, T., "Gas diffusion over an isolated hill under neutral, stable and unstable conditions', Atmospheric Environment, vol. 36, 5697-5707, 2002.

Ohya, Y., Nakamura, Y. and Ozono, S.; A wind tunnel for studying density-stratified flows, Atmospheric Environment, 28, 1895-1900, 1994.

Ross, A. N., Arnold, S., Vosper, S. B., Mobbs, S. D., Nixon, N. and Robins, A. G.: "A comparison of wind-tunnel experiments and numerical simulations of neutral and stratified flow over a hill", Boundary Layer Meteorology, vol. 113, 427-459, 2004.

Schlichting, H.; "Boundary-layer theory", Mc-Graw Hill, 1979.

Sheppard, P. A.; "Flow over mountains", Quart. J. Roy. Meteor. Soc., 82, 528-529, 1956.

Smith, R. B.; "Why can't stably stratified air rise over high ground?" In Atmospheric Processes over Complex Terrain. Meteorological Monographs, 35, American Meteorological Society, Boston, MA, 105-107, 1990.

Snyder, W. H., Thompson, R. S., Eskridge, R. E., Lawson, R. E., Castro, I. P., Lee, J. T., Hunt, J. C. R. and Ogawa, Y.; "The Structure of Strongly Stratified Flow over Hills: Dividing Streamline Concept", J. Fluid Mechanics, 152, 249-288, 1985.

Sykes, R.I., "Stratified Flows over Low Hills", Proc. R. Soc. London A, Vol. 361, pp. 225-243, 1978.

Taylor, P. A., "Numerical Studies of Neutrally Stratified Planetary Boundary Layer over Gentle Topography", Boundary-layer Meteorology, vol. 12, 37-60, 1997.

Teunissen, H. W.; "Wind--tunnel and Full--scale Comparisons of Mean Wind Flow Over an Isolated Low Hill", J. Wind Eng. Ind. Aerodynamics, vol. 15, 271-286, 1983.

Townsend, A. A.; "Structures of Turbulent Shear Flow", Cambridge University Press, 1976.

Zeman, O. and Jensen, N. O.; "Modification of turbulence characteristics in flow over hills", Q. J. R. Meteorol. Soc., vol. 113, 55-80, 1987.